ChemComm

COMMUNICATION

View Article Online
View Journal





Cite this: DOI: 10.1039/d0cc07821b

Received 1st December 2020,
Accepted 15th December 2020

DOI: 10.1039/d0cc07821b

rsc.li/chemcomm

# Real-time monitoring of caspase-3/8 activity by self-assembling nanofiber probes in living cells†

Li-Song Zhang,[a] Hong-Lei Xu,[a] Ying Xia,[a] Jian-Peng Bi,[a] Chuan-Zeng Zhang,[a] Zhen Xi,[b] Lu-Yuan Li[a] and Zhi-Song Zhang *[a]

**Caspase-3/8 are key members of the cysteine–aspartyl protease family with pivotal roles in apoptosis. We have designed and synthesized self-assembling probes, Nap-GFFpYDEVD-AFC and Nap-GFFpYIETD-AFC, with fluorescence 'turn-on' properties for real-time monitoring of Caspase-3/8 activity in living cells.**

Apoptosis, the major type of programmed cell death, is a highly regulated process involved in tissue and organ development, immune system functions, and many diseases including cancer.[1–4] Dysregulated apoptosis may lead to tumorigenesis and cancer drug resistance.[5,6] A number of factors may induce a cascade of apoptotic signals leading to pathological changes in cells such as DNA breakage and protein degradation.[7,8] The caspase family of proteins play an important role in this process. Caspases are usually synthesized as inactive zymogens which when cells respond to cell death or inflammatory stimuli convert to their active forms.[9] At the onset of apoptosis the initiator caspase is activated and, in turn, cleaves and activates the effector caspases to catalyze proteolysis of respective protein substrates.[4] Caspase-8 and Caspase-3 are a typical pair of initiator caspase and effector caspase that are activated sequentially, and the activation status of these two enzymes is a quintessential mark for classic apoptosis.[1,10–12] Therefore, there is an urgent need for rapid and real-time monitoring of this process in biomedical research as well as in clinical applications.

The detection of caspase activities, unlike analyses of DNA fragmentation or cell membrane phospholipids, not only reflects the intensity of the apoptotic process at an earlier stage, but also quickly identifies apoptotic signalling pathways the cell utilizes.[13] Short peptide sequences on the substrates of caspase enzymes have been reported, such as IETD and DEVD for Caspase-8 and Caspase-3,[14–16] respectively, to aid the detection of caspase activities. Fluorescent group such as 7-amino-4-trifluoromethylcoumarin (AFC), which has a fluorescent property depending on the electron donating ability of the 7-amino group, has been utilized to modify peptidyl substrates of caspases,[17–19] such that the highly fluorescent group AFC is released when the amide bond between the peptide and the coumarin is cleaved, as in the cases of Ac-DEVD-AFC and Ac-IETD-AFC that are used for detecting Caspase-3 and Caspase-8 activities in cell lysates.[20,21] However, these probes cannot be readily used for real-time detection of apoptosis in living cells because of their poor ability to penetrate membrane of living cells.

In this study, we designed and synthesized fluorescent probes Nap-GFFpYDEVD-AFC and Nap-GFFpYIETD-AFC for the detection of activated caspases in living cells. Results show that when catalysed by alkaline phosphatase (ALP), which is widely distributed on the cell surface,[22] the Nap-GFFpY moiety promotes self-assembly of the probes to form nanofibers, which enter the cell through endocytosis at high efficiency.[22] Activated Caspase-8/3 will then recognize IETD/DEVD sequences, cleave the probes, and release the AFC groups. The fluorescence intensity of the free AFC is proportional to the activity of the corresponding caspase in the cytoplasm (Scheme 1).

The details of syntheses of Nap-GFFpYDEVD-AFC, Nap-GFFpYIETD-AFC, Nap-GFFYDEVD-AFC and Nap-GFFYIETD-AFC are given in the ESI,† (Fig. S1). Fmoc-Asp(OH)-AFC was synthesized in two steps with a total yield of 73%[19](Fig. S1, ESI†). Nap-GFFpYDEVD-AFC, Nap-GFFpYIETD-AFC, Nap-GFFYDEVD-AFC and Nap-GFFYIETD-AFC were prepared by standard Fmoc solid phase peptide synthesis (SPPS) using 2-chlorotrityl chloride resin and the corresponding N-Fmoc protected amino acid as previously described[23] (Fig. 1A and Fig. S1, ESI†). The carboxyl group was deprotected with 95% trifluoroacetic acid and cleaved from the resin to produce Nap-GFFpYDEVD-AFC, Nap-GFFpYIETD-AFC, Nap-GFFYDEVD-AFC and Nap-GFFYIETD-AFC as described,[24] which were further purified by high performance liquid chromatography (HPLC). The chemical synthesis route of ALP inhibitor (DQB)[25] is shown in Fig. S2 (ESI†). The structures of the products were

[a] State Key Laboratory of Medicinal Chemical Biology, College of Pharmacy and Tianjin Key Laboratory of Molecular Drug Research, NanKai University, Tianjin 300350, China. E-mail: zzs@nankai.edu.cn
[b] Key Laboratory of Elemento-Organic Chemistry and College of Chemistry, Nankai University, 94 Weijin Road, Tianjin 300071, China

† Electronic supplementary information (ESI) available. See DOI: 10.1039/d0cc07821b

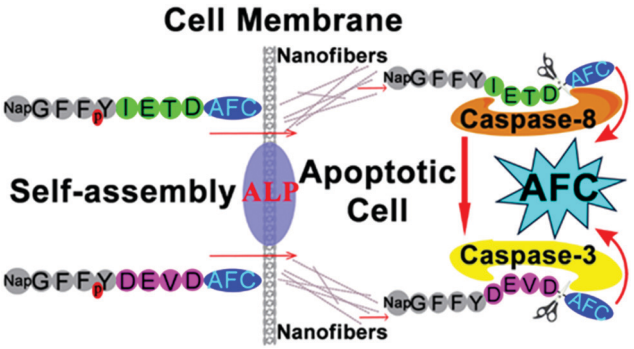


Scheme 1 Schematic of the mechanism of Nap-GFFpYIETD-AFC and Nap-GFFpYDEVD-AFC imaging of Caspase-8 and Caspase-3 activity in apoptotic tumour cells.

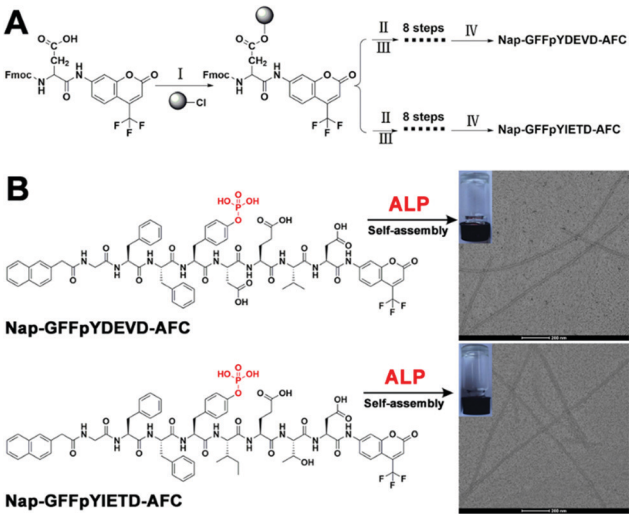


Fig. 1 (A) Synthesis route of Nap-GFFpYDEVD-AFC and Nap-GFFpYIETD-AFC. (B) TEM images of the hydrogels formed by 5 mmol $L^{-1}$ Nap-GFFpYDEVD-AFC and Nap-GFFpYIETD-AFC probes with addition of ALP (2.0 U $mL^{-1}$) at pH = 7.4. Inset: Optical images. Scale bar: 100 nm.

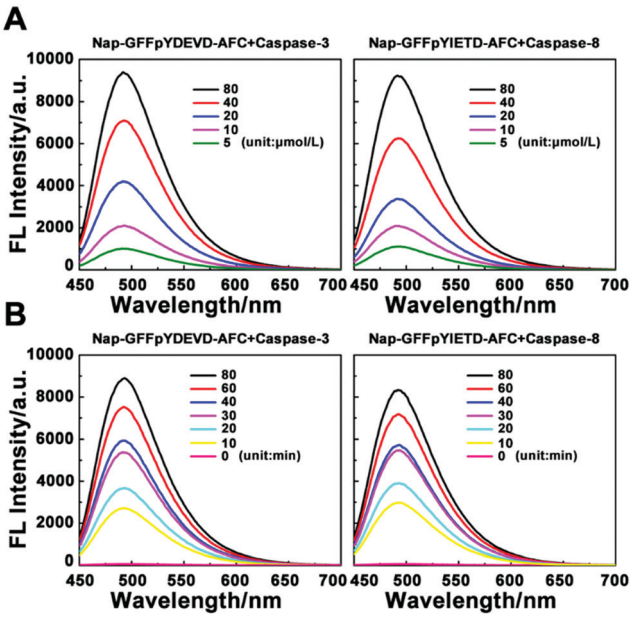


Fig. 2 Nap-GFFpYDEVD-AFC and Nap-GFFpYIETD-AFC are catalyzed by recombinant human Caspase-3/8 protein to release AFC. (A) Concentration gradient release culve: AFC fluorescence test results of Nap-GFFpYDEVD-AFC and Nap-GFFpYIETD-AFC at different concentrations (5, 10, 20, 40, 80 μmol $L^{-1}$) after catalysis by recombinant Caspase-3/8 protein for 120 min. (B) Time gradient release culve: AFC fluorescence test results of Nap-GFFpYDEVD-AFC and Nap-GFFpYIETD-AFC (40 μmol $L^{-1}$) after hydrolysed by recombined Caspase-3/8 protein for different period of time (0, 10, 20, 30, 40, 60, 80 min).

confirmed by NMR spectroscopy analysis and shown in Fig. S3A–S8B (ESI†).

For the solubility of the probes, Nap-GFFpYDEVD-AFC and Nap-GFFpYDEVD-AFC at 10 mmol $L^{-1}$ in PBS (pH 7.4) form clear solutions due to the presence of the phosphate group in the anionic form (Fig. S9, ESI†). However, the solubility of probes without the phosphate group significantly decreases (Fig. S9, ESI†). Addition of recombinant ALP (2.0 U $mL^{-1}$, 37 °C) lead to self-assembly of the probes to form nanofibers with a diameter of about 10 nm (Fig. 1B), measured with a transmission electron microscopy (TEM). The self-assembled nanofiber hydrogel remains stable for more than 15 days at 37 °C.

We used a fluorescence spectrophotometer to test the excitation and emission wavelengths of the free AFC and the self-assembled probes. After AFC dissociated from the probes, the maximum excitation wavelength is red-shifted from 384 nm to 440 nm, and the maximum emission wavelength is red-shifted from 440 nm to 492 nm. The fluorescence intensity of free AFC also increased significantly at the same concentration (Fig. S10A–D, ESI†). The strong fluorescence of AFC can be observed at the excitation wavelength of 440 nm, but the fluorescence of the probe itself is not observed at all (Fig. S10E, ESI†). Therefore, under the excitation wavelength of 458 nm of the confocal microscope, the activity of Caspase-3 and Caspase-8 protein in living cells can be detected because of the fluorescence intensity of the freed AFC.

We determined the direct interaction between self-assembled peptide probes Nap-GFFpYDEVD-AFC or Nap-GFFpYIETD-AFC and the corresponding recombinant human Caspase-3 or Caspase-8 proteins. In 120 min, the curves in Fig. 2A exhibit positive correlation between probe concentration and free AFC fluorescence intensity. When the concentration of probes was maintained at 40 μmol $L^{-1}$, the fluorescence intensity of free AFC gradually increased with the prolonging of the action time of corresponding Caspase protein (Fig. 2B). These *in vitro* enzymatic assays demonstrate that Caspase-3 recognizes the DEVD sequence in the probe Nap-GFFpYDEVD-AFC and Caspase-8 recognizes the IETD sequence in the probe Nap-GFFpYIETD-AFC. Both self-assembled probes exhibit the breakage of the amide bond between aspartic acid and AFC, releasing the fluorescent group AFC.

We treated cervical cancer HeLa cells and breast cancer MCF-7 cells with the two probes at the concentrations up to 200 μmol $L^{-1}$ for 48 hours. Analysis of the treated cells by MTT

 

and flow cytometry based Anexin-V assays indicated that the treatment did not induce any significant cytotoxicity or apoptosis (Fig. S11 and S12, ESI†), suggesting good biocompatibility of the probes.

We then determined the ability of the two probes to detect apoptotic signals in HeLa and MCF-7 cell cultures. The cells were treated with either Nap-GFFpYDEVD-AFC or Nap-GFFpYIETD-AFC (50 μmol $L^{-1}$, 4 hours), using Ac-DEVD-AFC or Ac-IETD-AFC, respectively, in control experiments. Confocal laser scanning microscopic analysis of the cells showed only marginal fluorescent background. Upon the addition of $H_2O_2$ (1 mmol $L^{-1}$), which induces apoptosis,[14,26] the blue-green fluorescence from free AFC emerged and the fluorescence intensity became stronger with time, clearly indicating the occurrence of apoptosis in the cells (Fig. 3 and Fig. S14, ESI†). Cells treated with either Ac-DEVD-AFC or Ac-IETD-AFC showed no fluorescence after 60 minutes of $H_2O_2$ treatment (Fig. S13, ESI†). These findings indicate that self-assembly into nanofibers is a prerequisite for efficient cellular uptake of the probes.

We designed a siRNA that was capable of knock down ALP protein on the surface of tumor cells. Western Blotting analysis results show that ALP siRNA can significantly reduce the expression of ALP protein on the cell membrane surface in MCF-7 and HeLa cells (Fig. S15, ESI†). During the process of apoptosis of MCF-7 cells and HeLa cells induced by hydrogen peroxide, using a confocal microscope, we show that the fluorescence brightness of AFC in the two living cells decreased significantly after siRNA-treatment, similar to the results from alkaline phosphatase inhibitor treatments (Fig. S16 and S17, ESI†). These findings indicate that inhibiting the activity of ALP of tumor cells significantly reduces the efficiency of self-assembled probes entering into the cells.

We determined the specificity of the two probes for the caspase cascade by using selective inhibitors of Caspase-8 and Caspase-3, Z-IETD-FMK and Z-DEVD-FMK, respectively (Fig. 4 and Fig. S18, ESI†). Results showed that Z-DEVD-FMK nearly completely prevented Caspase-3-catalyzed proteolysis of Nap-GFFpYDEVD-AFC, but that of Nap-GFFpYIETD-AFC. On the other hand, Z-IETD-FMK inhibited Caspase-8-catalyzed proteolysis of Nap-GFFpYIETD-AFC and Nap-GFFpYDEVD-AFC, when

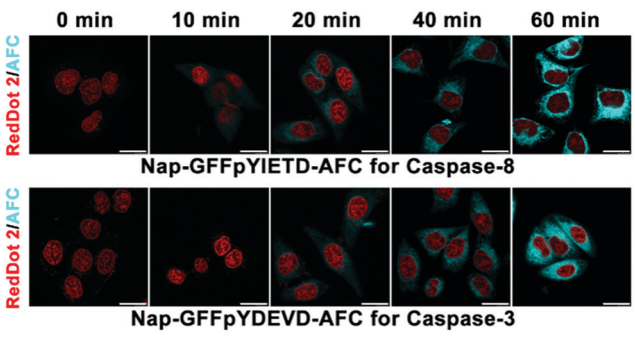


Fig. 3 Confocal images of HeLa cells incubated with 50 μmol $L^{-1}$ Nap-GFFpYDEVD-AFC or Nap-GFFpYIETD-AFC for 4 h and further treated with $H_2O_2$ (1.0 mmol $L^{-1}$). AFC: $\lambda_{ex}$ = 458 nm, $\lambda_{em}$ = 492 nm, RedDot 2: $\lambda_{ex}$ = 561 nm, $\lambda_{em}$ = 700 nm. Scale bar: 20 μm.

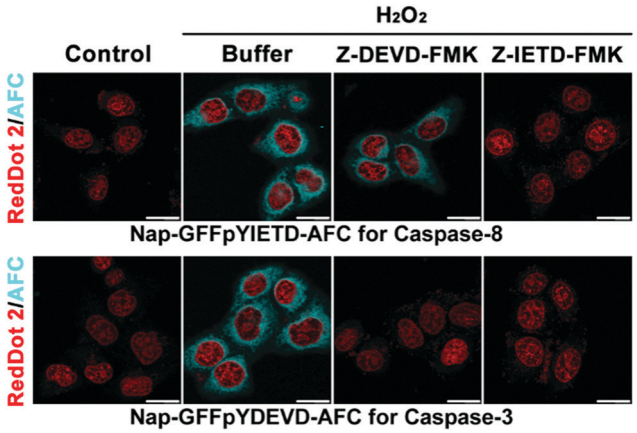


Fig. 4 Confocal images of HeLa cells incubated with Nap-GFFpYDEVD-AFC or Nap-GFFpYIETD-AFC (50 μmol $L^{-1}$) and Caspase-8/3 inhibitors for 2 h with or without further treatment by $H_2O_2$ (1.0 mmol $L^{-1}$). AFC: $\lambda_{ex}$ = 458 nm, $\lambda_{em}$ = 492 nm, RedDot 2: $\lambda_{ex}$ = 561 nm, $\lambda_{em}$ = 700 nm. Scale bar: 20 μm.

the cells were treated with $H_2O_2$. These findings indicate that our probes are highly specific toward the intended caspases, thus appropriate for the detection of the apoptotic signals in living cells.

One apparent application of these probes is for high throughput screening of drug candidates that induce apoptosis in cancer cells. We treated HeLa cells with either of the two caspase-responsive fluorescent probes in the presence or absence of one of the clinically used anti-cancer drugs, namely, taxol (5 μmol $L^{-1}$), doxorubicin (5 μmol $L^{-1}$), etoposide (20 μmol $L^{-1}$) and cisplatin (10 μmol $L^{-1}$) (Fig. 5). After 3 hours of incubation, the fluorescence intensity of the cell cultures was measured by using a confocal laser scanning microscope. AFC fluorescence was detected in all of the drug-treated cells, indicating the activation of the apoptosis process. We repeated the experiments with MCF-7 cells and obtained similar results (Fig. S19, ESI†). These data demonstrate the utility of the two probes in rapid evaluation of the activities of cancer drugs.

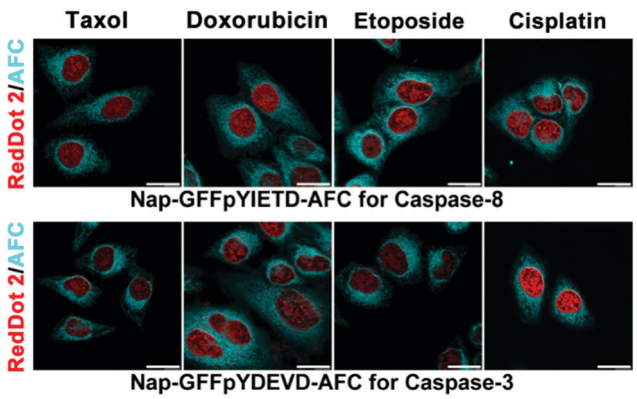


Fig. 5 HeLa cells were co-incubated with Nap-GFFpYDEVD-AFC or Nap-GFFpYIETD-AFC and 4 commonly used anticancer drugs, taxol (5 μmol $L^{-1}$), doxorubicin (5 μmol $L^{-1}$), etoposide (20 μmol $L^{-1}$) and cisplatin (10 μmol $L^{-1}$), the fluorescence of AFC were observed. AFC: $\lambda_{ex}$ = 458 nm, $\lambda_{em}$ = 492 nm, RedDot 2: $\lambda_{ex}$ = 561 nm, $\lambda_{em}$ = 700 nm. Scale bar: 20 μm.

In summary, we have developed fluorescence-generating, self-assembling nanofiber probes Nap-GFFpYDEVD-AFC and Nap-GFFpYIETD-AFC for the analysis of apoptosis in living cells. The formation of the nanofibers facilitate the uptake of the probes by the cells. Once taken up by the cells, the probes can be used to monitor the activation of either Caspase-3 or Caspase-8 in real-time, assisting the dissection of apoptosis signals, such as the activation of Caspase-8 and subsequent activation of Caspase-3. It is worth noting that the molecular structures of these probes can be modified by replacing the characteristic peptide sequences of the substrates recognized by other caspases or proteases, thus opening up new avenues for real-time imaging applications for a wide variety of biological processes.

This work was financial supported by National Natural Science Foundation of China (NSFC) projects (grant no. 81672740, 81972687 and 81874167).

## Conflicts of interest

There are no conflicts to declare.

## Notes and references

1 R. C. Taylor, S. P. Cullen and S. J. Martin, *Nat. Rev. Mol. Cell Biol.*, 2008, **9**, 231–241.
2 T. Bergsbaken, S. L. Fink and B. T. Cookson, *Nat. Rev. Microbiol.*, 2009, **7**, 99–109.
3 F. Elvas, T. V. Berghe, Y. Adriaenssens, P. Vandenabeele, K. Augustyns, S. Staelens, S. Stroobants, P. Van der Veken and L. Wyffels, *Org. Biomol. Chem.*, 2019, **17**, 4801–4824.
4 J. Xiao, P. Broz, A. W. Puri, E. Deu, M. Morell, D. M. Monack and M. Bogyo, *J. Am. Chem. Soc.*, 2013, **135**, 9130–9138.
5 S. Arguelles, A. Guerrero-Castilla, M. Cano, M. F. Munoz and A. Ayala, *Ann. N. Y. Acad. Sci.*, 2019, **1443**, 20–33.
6 C. J. Vickers, G. E. Gonzalez-Paez and D. W. Wolan, *J. Am. Chem. Soc.*, 2013, **135**, 12869–12876.
7 H. Shi, R. T. Kwok, J. Liu, B. Xing, B. Z. Tang and B. Liu, *J. Am. Chem. Soc.*, 2012, **134**, 17972–17981.
8 Y. Shi, *Nat. Struct. Biol.*, 2001, **8**, 394–401.
9 E. M. Creagh, H. Conroy and S. J. Martin, *Immunol. Rev.*, 2003, **193**, 10–21.
10 J. M. Buschhaus, B. Humphries, K. E. Luker and G. D. Luker, *Cells*, 2018, 7.
11 C. Gunther, E. Martini, N. Wittkopf, K. Amann, B. Weigmann, H. Neumann, M. J. Waldner, S. M. Hedrick, S. Tenzer, M. F. Neurath and C. Becker, *Nature*, 2011, **477**, 335–339.
12 Y. Wang, X. Hu, J. Weng, J. Li, Q. Fan, Y. Zhang and D. Ye, *Angew. Chem., Int. Ed.*, 2019, **58**, 4886–4890.
13 X. Liu, X. Song, D. Luan, B. Hu, K. Xu and B. Tang, *Anal. Chem.*, 2019, **91**, 5994–6002.
14 Y. Yuan, C. J. Zhang, R. T. K. Kwok, D. Mao, B. Z. Tang and B. Liu, *Chem. Sci.*, 2017, **8**, 2723–2728.
15 H. Li, G. Parigi, C. Luchinat and T. J. Meade, *J. Am. Chem. Soc.*, 2019, **141**, 6224–6233.
16 G. Liang, H. Ren and J. Rao, *Nat. Chem.*, 2010, **2**, 54–60.
17 D. Kovacs, X. Lu, L. S. Meszaros, M. Ott, J. Andres and K. E. Borbas, *J. Am. Chem. Soc.*, 2017, **139**, 5756–5767.
18 Z. Xu, X. Liu, J. Pan and D. R. Spring, *Chem. Commun.*, 2012, **48**, 4764–4766.
19 S. Mizukami, R. Takikawa, F. Sugihara, M. Shirakawa and K. Kikuchi, *Angew. Chem., Int. Ed.*, 2009, **48**, 3641–3643.
20 X. Wang, X. He, S. Hu, A. Sun and C. Lu, International journal of experimental cellular physiology, biochemistry, and pharmacology, *Cell. Physiol. Biochem.*, 2015, **35**, 1527–1536.
21 P. Reszka, R. Schulz, K. Methling, M. Lalk and P. J. Bednarski, *ChemMedChem*, 2010, **5**, 103–117.
22 H. He, S. Liu, D. Wu and B. Xu, *Angew. Chem., Int. Ed.*, 2020, **59**, 16445–16450.
23 I. Coin, M. Beyermann and M. Bienert, *Nat. Protoc.*, 2007, **2**, 3247–3256.
24 C. Ornelas, J. Broichhagen and M. Weck, *J. Am. Chem. Soc.*, 2010, **132**, 3923–3931.
25 R. Dahl, E. A. Sergienko, Y. Su, Y. S. Mostofi, L. Yang, A. M. Simao, S. Narisawa, B. Brown, A. Mangravita-Novo, M. Vicchiarelli, L. H. Smith, W. C. O'Neill, J. L. Millan and N. D. Cosford, *J. Med. Chem.*, 2009, **52**, 6919–6925.
26 Y. Wu, D. Wang, X. Wang, Y. Wang, F. Ren, D. Chang, Z. Chang and B. Jia, *Cell. Physiol. Biochem.*, 2011, **27**, 539–546.

 